Stability analysis of fixed point of fractional-order coupled map lattices

Sachin Bhalekar[a], Prashant M. Gade[b]

[a]*School of Mathematics and Statistics, University of Hyderabad, Hyderabad, 500046 India*
[b]*Department of Physics, RTM Nagpur University, Nagpur*

Abstract

We study the stability of synchronized fixed-point state for linear fractional-order coupled map lattice(CML). We observe that the eigenvalues of the connectivity matrix determine the stability as for integer-order CML. These eigenvalues can be determined exactly in certain cases. We find exact bounds in one-dimensional lattice with translationally invariant coupling using the theory of circulant matrices. This can be extended to any finite dimension. Similar analysis can be carried out for the synchronized fixed point of non-linear coupled fractional maps where eigenvalues of the Jacobian matrix play the same role. The analysis is generic and demonstrates that the eigenvalues of connectivity matrix play a pivotal role in stability analysis of synchronized fixed point even in coupled fractional maps.

1. Introduction

Fractional dynamics extends the dynamical systems to systems with memory and studies in fractional order differential equations have exploded in the recent past. In integer-order systems, dynamical systems theory has been enriched by studies in flows as well as maps. Numerical difficulties are almost absent in the simulation of maps. Almost all routes to chaos observed in flows are observed in maps as well [1]. Most chaos control schemes are applicable in the flows as well as maps. They appear naturally in scientific contexts where time is discrete. They have found applications in convecting

Email addresses: `sachin.math@yahoo.co.in, sachinbhalekar@uohyd.ac.in (Corresponding Author)` (Sachin Bhalekar), `prashant.m.gade@gmail.com` (Prashant M. Gade)

fluids, lasers, heart cells, chemical oscillators, etc [2]. Circle map has found applications in several systems described by a damped driven pendulum. Examples include Josephson junction in microwave field [3], charge density waves, lasers [4, 5] cardiac arrhythmia [6] and even air-bubble formation [7]. Logistic maps have found applications in chemical physics and population dynamics [8, 9] These systems have been extended to a spatially extended version popularly known as coupled map lattice. Coupled map lattices have found applications in diverse fields such as austenite-martensite structural transformation, convection and crystal growth [10, 11, 12].

Thus it can be useful to investigate coupled fractional maps to understand the dynamics of spatiotemporal systems in presence of memory. Studies in fractional maps are unfrequent compared to fractional differential equations. Simulation of the fractional differential equation is computationally cumbersome compared to ordinary differential equation. It also needs domain expertise in numerical analysis. Simulating high dimensional system of fractional differential equations will need extensive computational resources. Though simulation of fractional maps is more time-consuming than integer-order maps, the computational resources required are far less than that for fractional differential equations.

Systems with power-law memory occur in several physical situations ranging from electromagnetic waves in dielectric media to adaptation in biological systems [13, 14]. In this work, we study coupled fractional maps and investigate a very basic problem of existence and stability of fixed-point solution and state conditions for a synchronized fixed-point solution. In certain important cases, such as coupled map lattice in finite dimension, explicit bounds can be derived for stability.

2. Preliminaries

In this section, we present some basic definitions and results. Let $h > 0$, $a \in \mathbb{R}$, $(h\mathbb{N})_a = \{a, a+h, a+2h, \ldots\}$ and $\mathbb{N}_a = \{a, a+1, a+2, \ldots\}$.

Definition 2.1. *(see [15, 16, 17]). For a function $x : (h\mathbb{N})_a \to \mathbb{R}$, the forward h-difference operator if defined as*

$$(\Delta_h x)(t) = \frac{x(t+h) - x(t)}{h},$$

where $t \in (h\mathbb{N})_a$.

Throughout this paper, we take $a = 0$ and $h = 1$.

Definition 2.2. *[17] For a function $x : \mathbb{N}_\circ \to \mathbb{R}$ the fractional sum of order $\alpha > 0$ is given by*

$$(\Delta^{-\alpha} x)(t) = \frac{1}{\Gamma(\alpha)} \sum_{s=0}^{n} \frac{\Gamma(\alpha + n - s)}{\Gamma(n - s + 1)} x(s), \tag{1}$$

where, $t = \alpha + n,\ n \in \mathbb{N}_\circ$.

Definition 2.3. *[17, 18] Let $\mu > 0$ and $m - 1 < \mu < m$, where $m \in \mathbb{N}$, $m = \lceil \mu \rceil$. The μth fractional Caputo like difference is defined as*

$$\Delta^{\mu} x(t) = \Delta^{-(m-\mu)} \left(\Delta^{m} x(t) \right), \tag{2}$$

where $t \in \mathbb{N}_{m-\mu}$ and

$$\Delta^{m} x(t) = \sum_{k=0}^{m} \binom{m}{k} (-1)^{m-k} x(t + k). \tag{3}$$

Definition 2.4. *[17] The Z-transform of a sequence $\{y(n)\}_{n=0}^{\infty}$ is a complex function given by $Y(z) = Z[y](z) = \sum_{k=0}^{\infty} y(k) z^{-k}$ where $z \in \mathbb{C}$ is a complex number for which the series converges absolutely.*

Definition 2.5. *[17] Let $\tilde{\phi}_\alpha(n)$ be a family of binomial functions defined on $\mathbb{Z}$, parametrized by α defined by*

$$\begin{aligned} \tilde{\phi}_\alpha(n) &= \frac{\Gamma(n + \alpha - 1)}{\Gamma(\alpha)\Gamma(n)} \\ &= \begin{pmatrix} n + \alpha - 1 \\ n \end{pmatrix} = (-1)^{n} \begin{pmatrix} -\alpha \\ n \end{pmatrix}. \end{aligned} \tag{4}$$

Then

$$Z(\tilde{\phi}_\alpha(t)) = \frac{1}{(1 - z^{-1})^{\alpha}}, \quad |z| > 1.$$

Definition 2.6. *[17] The convolution $\phi * x$ of the functions ϕ and x defined on $\mathbb{N}$ is defined as*

$$\left(\phi * x \right)(n) = \sum_{s=0}^{n} \phi(n - s) x(s) = \sum_{s=0}^{n} \phi(s) x(n - s).$$

Then the Z-transform of this convolution is

$$Z \left(\phi * x \right)(n) = \left(Z \left(\phi \right)(n) \right) \left(Z \left(x \right)(n) \right). \tag{5}$$

Lemma 2.1. *[18] The discrete function $x(t)$ is solution of an initial value problem*

$$\begin{aligned} \Delta^\alpha x(t) &= f(x(t+\alpha-1)), \quad t \in N_{1-\alpha}, \quad 0<\alpha<1, \\ x(0) &= x_0 \end{aligned} \tag{6}$$

if and only if $x(t)$ is solution of following fractional discrete dynamical system

$$\begin{aligned} x(t) &= x_0 + \sum_{s=1-\alpha}^{t-\alpha} \frac{\Gamma(t-s)}{\Gamma(\alpha)\Gamma(t-s-\alpha+1)} f\left(x(s+\alpha-1)\right) \\ &= x_0 + \sum_{j=0}^{t-1} \frac{\Gamma(t-j+\alpha-1)}{\Gamma(\alpha)\Gamma(t-j)} f\left(x(j)\right). \end{aligned} \tag{7}$$

3. Fractional order coupled map lattices: Linear systems

Consider the linear coupled map lattice of fractional order $\alpha \in (0,1)$

$$x_{t+1}(k) = x_0(k) + \sum_{j=0}^{t}\sum_{m=1}^{N} \frac{\Gamma(t-j+\alpha)}{\Gamma(\alpha)\Gamma(t-j+1)} \left(A_{km}x_j(m) - x_j(k)\right), \tag{8}$$

where $x_t(k)$ is the variable at time t associated with the k-th lattice point, $k = 1, 2, \cdots, N$, $x_t(0) = x_t(N)$ and $x_t(N+1) = x_t(1)$ and $A = (A_{km})$ is $N \times N$ connectivity matrix.
If we write $X_t = (x_t(1), x_t(2), \cdots, x_t(N))$, a column vector in $\mathbb{R}^N$ then the system (8) is equivalent to

$$\begin{aligned} X_{t+1} &= X_0 + \sum_{j=0}^{t} \frac{\Gamma(t-j+\alpha)}{\Gamma(\alpha)\Gamma(t-j+1)} (A-I)\, X_j, \\ &= X_0 + (A-I)\left(\tilde{\phi}_\alpha(t) * X_t\right), \end{aligned} \tag{9}$$

where I is $N \times N$ identity matrix. Applying Z-transform and using the properties given in Section 2, we get

$$z\bar{X}(z) - zX_0 = \frac{1}{1-z^{-1}} X_0 + \frac{1}{(1-z^{-1})^\alpha} \bar{X}(z)\,(A-I), \quad |z|>1,$$

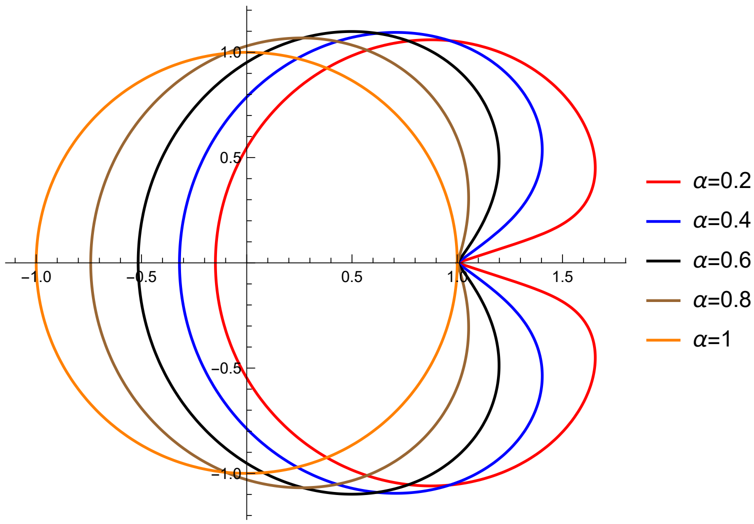

Figure 1: The stability region of fractional order map

where $\bar{X}(z)$ is the Z-transform of X_t. Therefore, the characteristic equation of system (9) is given as

$$det\left(z(1-z^{-1})^{\alpha}I-(A-I)\right)=0. \tag{10}$$

Motivated from [19, 20], we propose the following stability theorem.

Theorem 3.1. *The zero solution of the system (8) or (9) is asymptotically stable if and only if all the roots of the characteristic equation (10) satisfy* $|z|<1$.

3.1. Stable Region

At the boundary of stable region, the root z of characteristic equation (10) should satisfy $|z|=1$. Therefore, we obtain the parametric boundary curve $\beta(t)$ of stable region by substituting $z=e^{\iota t}$, $0\le t\le 2\pi$ in the (10) as

$$\beta(t)=\left(2^{\alpha}\left(\sin(t/2)\right)^{\alpha}\cos\left(\alpha\frac{\pi}{2}+t(1-\alpha/2)\right)+1, 2^{\alpha}\left(\sin(t/2)\right)^{\alpha}\sin\left(\alpha\frac{\pi}{2}+t(1-\alpha/2)\right)\right). \tag{11}$$

The boundary curves $\beta(t)$ for different values of $\alpha\in(0,1]$ are sketched in Figure 1. If the eigenvalues of A are complex, we need to consider if the given eigenvalue is in the stable region defined by the cardioid given above and the solution is stable only if all eigenvalues lie in the stable region.

We have following result [19, 21, 22, 20].

Theorem 3.2. *If all the eigenvalues of matrix A lie inside the region bounded by the curve $\beta(t)$, $0 \leq t \leq 2\pi$ defined by (11) then the system (8) is asymptotically stable.*

Thus the stability of synchronized fixed point $x_t(k) = 0$ as $t \to \infty$ $\forall i$ depends only on eigenvalues of connectivity matrix A. Let us consider a particular case of coupled map lattice on one-dimensional lattice with translationally invariant coupling and periodic boundary conditions. The matrix A such that $A_{ii} = a_1$, $A_{i,i+1} = a_2$ and $A_{i,i-1} = a_0$ is given by.

$$A = \begin{pmatrix} a_1 & a_2 & 0 & 0 & \cdots & 0 & 0 & a_0 \\ a_0 & a_1 & a_2 & 0 & \cdots & 0 & 0 & 0 \\ 0 & a_0 & a_1 & a_2 & \cdots & 0 & 0 & 0 \\ \vdots & \vdots & \vdots & \vdots & & \vdots & \vdots & \vdots \\ 0 & 0 & 0 & 0 & \cdots & a_0 & a_1 & a_2 \\ a_2 & 0 & 0 & 0 & \cdots & 0 & a_0 & a_1 \end{pmatrix}$$

For the special case $N = 2$, we define

$$A = \begin{pmatrix} a_1 & a_0 + a_2 \\ a_0 + a_2 & a_1 \end{pmatrix}$$

and for $N = 1$

$$A = \begin{pmatrix} a_1 + a_0 + a_2 \end{pmatrix}$$

using periodic boundary conditions.

A is a circulant matrix with eigenvalues $\lambda_l = a_1 + a_2\omega^l + a_0\omega^{-l}$ where $\omega = \exp(\iota\frac{2\pi}{N})$ is primitive Nth root of unity [23]. For symmetric case, where $a_2 = a_0$, we get $\lambda_l = a_1 + 2a_2\cos(\theta_l)$, where $\theta_l = \frac{2\pi l}{N}$ for $0 \leq l \leq N-1$. We note that $\lambda_l = \lambda_{N-l}$ in this case. For case $a_2 = -a_0$, we obtain $\lambda_l = a_1 + \iota 2a_2\sin(\theta_l)$ where $\theta_l = \frac{2\pi l}{N}$. If $N = 4K$, $\lambda_K = a_1 + \iota 2a_2$ and $\lambda_{3K} = a1 - \iota 2a2$. These are limiting cases in this system. Coupled map lattice in one dimension is a widely explored system and we will study the above cases in further detail in this section.

First we consider the bounds on real part of the eigenvalue.

Note: The stable region of the real eigenvalue λ is $1 - 2^\alpha < \lambda < 1$.

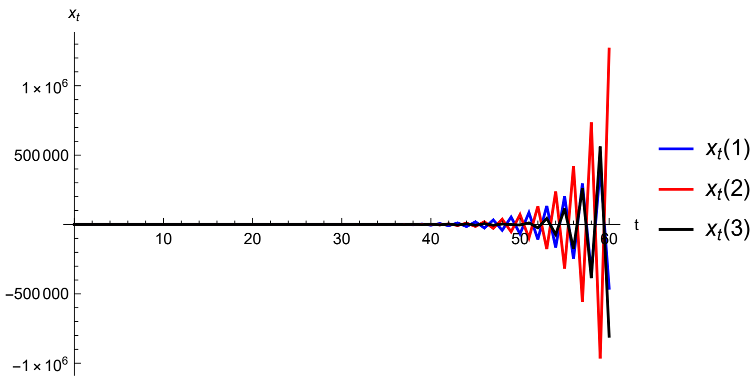

Figure 2: Unstable solution for $N = 3$, $\alpha = 0.4$, $a_0 = 0.2$, $a_1 = -0.5$ and $a_2 = 0.1$

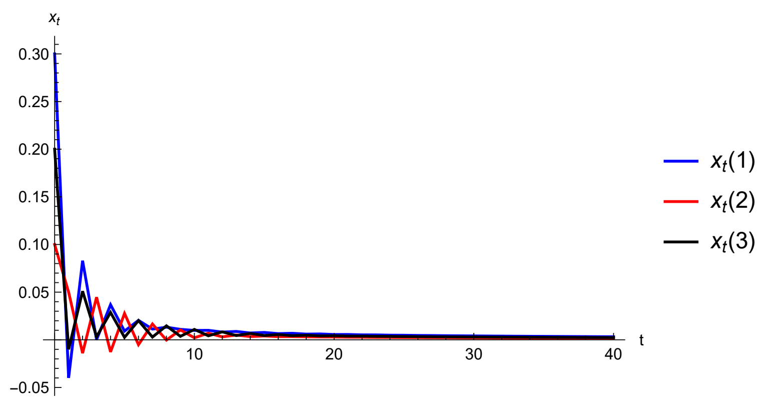

Figure 3: Stable solution for $N = 3$, $\alpha = 0.8$, $a_0 = 0.2$, $a_1 = -0.3$ and $a_2 = 0.1$

Example 3.1. *Consider $N = 3$ and $\alpha = 0.4$. The parameter values $a_0 = 0.2$, $a_1 = -0.5$ and $a_2 = 0.1$ produce the eigenvalues -0.2 and $-0.65 \pm 0.0866025\iota$. Since the eigenvalues $-0.65 \pm 0.0866025\iota$ are outside the stable region, we get the unstable solutions as shown in Fig. 2. On the other hand, if we set $N = 3$, $\alpha = 0.8$, $a_0 = 0.2$, $a_1 = -0.3$ and $a_2 = 0.1$ then all the eigenvalues viz. 0 and $-0.45 \pm 0.0866\iota$ lie inside the stable region and we get the stable solutions (cf. Fig. 3).*

In the following two subsections, we consider two important particular cases and discuss the stability.

3.1.1. Symmetric Case

In this section, we assume that the coefficient matrix A in (9) is symmetric i.e. $a_0 = a_2$.

Theorem 3.3. *The stable region of the system (9) with $a_0 = a_2$ is bounded by the quadrilateral with vertices $Q_1 = (0,1)$, $Q_2 = (-2^{\alpha-2}, 2^{\alpha-1} + 1 - 2^{\alpha})$, $Q_3 = (0, 1 - 2^{\alpha})$ and $Q_4 = (2^{\alpha-2}, 1 - 2^{\alpha-1})$ for even values of lattice points N and $Q_1 = (0,1)$, $Q_2' = \left(-\frac{2^{\alpha-1}}{1+\cos(\pi/N)}, \frac{2^{\alpha}}{1+\cos(\pi/N)} + 1 - 2^{\alpha}\right)$, $Q_3 = (0, 1 - 2^{\alpha})$ and $Q_4' = \left(\frac{2^{\alpha-1}}{1+\cos(\pi/N)}, -\frac{2^{\alpha}}{1+\cos(\pi/N)} + 1\right)$ for odd N in the a_2a_1-plane.*

Proof: The eigenvalues of A in the symmetric case are

$$\lambda_j = a_1 + 2a_2 \cos\left(\frac{2\pi j}{N}\right), \quad j = 0, 1, \cdots, N-1. \tag{12}$$

Note that $\cos\left(\frac{2\pi j}{N}\right) = \cos\left(\frac{2\pi(N-j)}{N}\right)$. Therefore, to obtain the distinct values we take $j = 0, 1, \cdots, [N/2]$, where $[r]$ is an integer-part of the real number r. Since, all these eigenvalues are real, the stable region in the a_2a_1-plane is an intersection of the regions

$$1 - 2^{\alpha} < a_1 + 2a_2 \cos\left(\frac{2\pi j}{N}\right) < 1, \quad j = 0, 1, \cdots, [N/2]. \tag{13}$$

The boundaries of these regions are straight lines defined by following two sets

$$S1_j: \quad a_1 = -2\cos\left(\frac{2\pi j}{N}\right) a_2 + (1 - 2^{\alpha}), \quad \text{and} \tag{14}$$

$$S2_j: \quad a_1 = -2\cos\left(\frac{2\pi j}{N}\right) a_2 + 1, \tag{15}$$

where $j = 0, 1, \cdots, [N/2]$.
Note that

$$[N/2] = \begin{cases} N/2, & \text{if } N \text{ is even} \\ (N-1)/2, & \text{if } N \text{ is odd.} \end{cases} \tag{16}$$

The stable region of (9) will be bounded by the straight lines $S1_j$ and $S2_j$ which are close to origin in the a_2a_1-plane, as shown in Figure 4. The lines in the set $S1_j$ intersect each other at $(0, 1 - 2^{\alpha})$ whereas those in the set

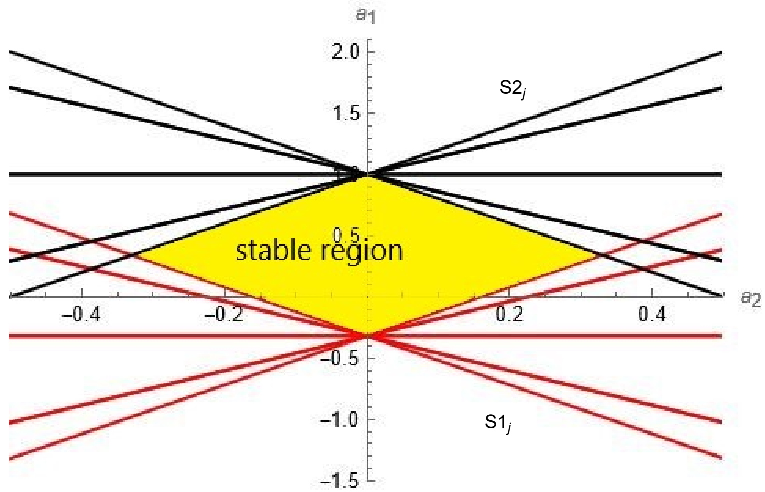

Figure 4: Stable region of symmetric case

$S2_j$ have intersection at $(0,1)$ in the a_2a_1-plane. Further, the innermost line $a_1 = -2a_2 + (1-2^{\alpha})$ in the set (14) with $j=0$ intersects the innermost line $a_1 = -2\cos\left(\frac{2\pi[N/2]}{N}\right)a_2 + 1$ in the set (15) with $j=[N/2]$ in the a_2a_1-plane at the point $(-2^{\alpha-2}, 2^{\alpha-1}+1-2^{\alpha})$ when N is even and at $\left(-\frac{2^{\alpha-1}}{1+\cos(\pi/N)}, \frac{2^{\alpha}}{1+\cos(\pi/N)}+1-2^{\alpha}\right)$ when N is odd. Secondly, the intersection between the innermost lines $a_1 = -2\cos\left(\frac{2\pi[N/2]}{N}\right)a_2+(1-2^{\alpha})$ in the set (14) with $j=[N/2]$ and $a_1 = -2a_2+1$ in the set (15) with $j=0$ is the point $(2^{\alpha-2}, 1-2^{\alpha-1})$ when N is even and $\left(\frac{2^{\alpha-1}}{1+\cos(\pi/N)}, -\frac{2^{\alpha}}{1+\cos(\pi/N)}+1\right)$ when N is odd.
Thus, the stable region which is an intersection of all the regions (13) is bounded by the quadrilateral with vertices described in the statement of this theorem. This proves the result.

We note that stable region does not change for even N. Two extreme values for $a_1+2a_2\cos(\theta_l)$ are given by $\lambda_0 = a_1+2a_2$ and $\lambda_{N/2} = a_1-2a_2$. For odd N, one of the limits $\lambda_0 = a_1+2a_2$ is still realized. Other limit is slightly bigger by a leading to a slightly higher stability range and the it is approached as $1/N^2$ for large N. Thus, in the thermodynamic limit $N\to\infty$, stability region for $N\to\infty$ coincides with stability region for $N=2$. Thus the stability of extreme eigenvalues in the thermodynamic limit determine

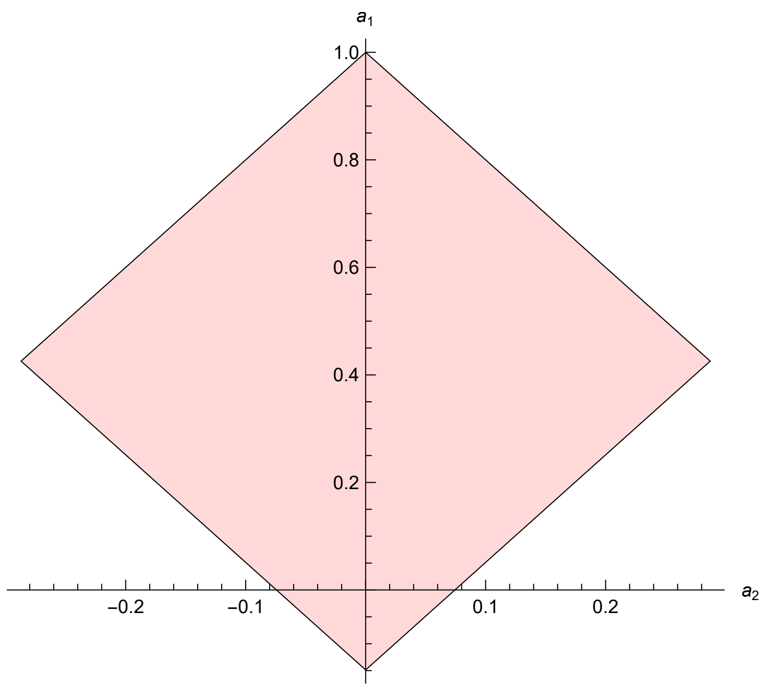

Figure 5: Stable region of symmetric system (9) with $N = 8$ and $\alpha = 0.2$

the stability region.

Example 3.2. *Consider the symmetric system (9) with even number $N = 8$ of lattice points and $\alpha = 0.2$. The stable region using Theorem 3.3 is sketched in Figure 5. We verified that the solutions starting in a neighborhood of origin converge to origin if we take (a_2, a_1) in the stable region. Figure 6 shows the converging trajectories for the parameter values $a_1 = 0.1$, and $a_2 = -0.05$. The unstable solution is sketched in Figure 7 with $a_1 = -0.02$, and $a_2 = 0.1$ which are outside the stable region.*

Example 3.3. *Let us consider the symmetric system (9) with odd number $N = 9$ of lattice points. The stable region in this case with $\alpha = 0.5$ is shown in Figure 8. The stable solution for the parameter values $a_1 = 0.6$, and $a_2 = -0.1$is shown in Figure 9 whereas the unstable solution for $a_1 = 0.2$, and $a_2 = 0.6$ is in Figure 10.*

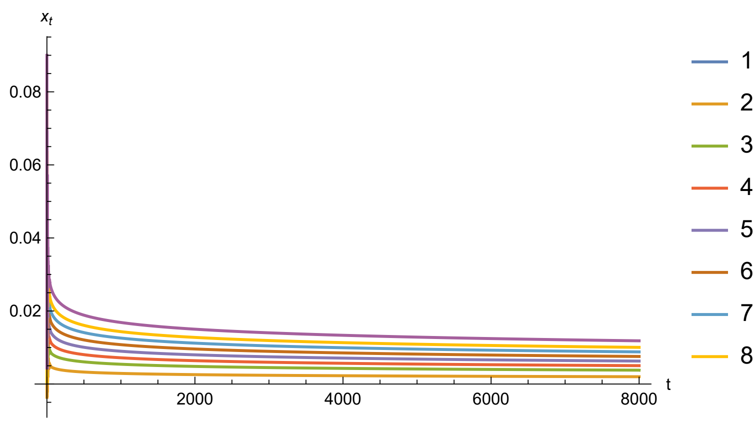

Figure 6: Stable solution of symmetric system (9) with $N = 8$, $\alpha = 0.2$, $a_1 = 0.1$, and $a_2 = -0.05$

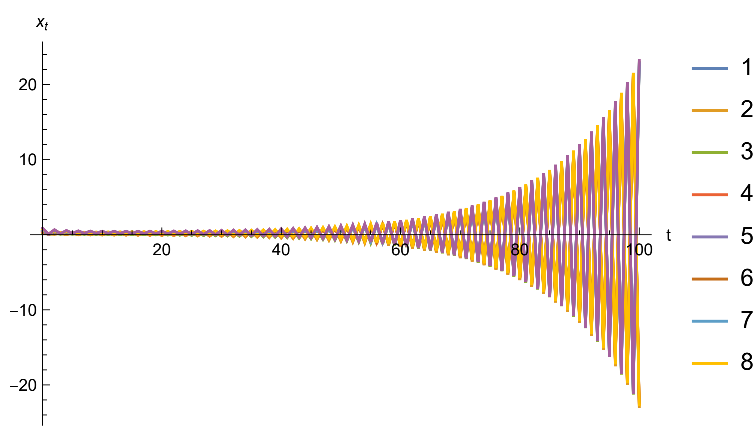

Figure 7: Unstable solution of symmetric system (9) with $N = 8$, $\alpha = 0.2$, $a_1 = -0.02$, and $a_2 = 0.1$

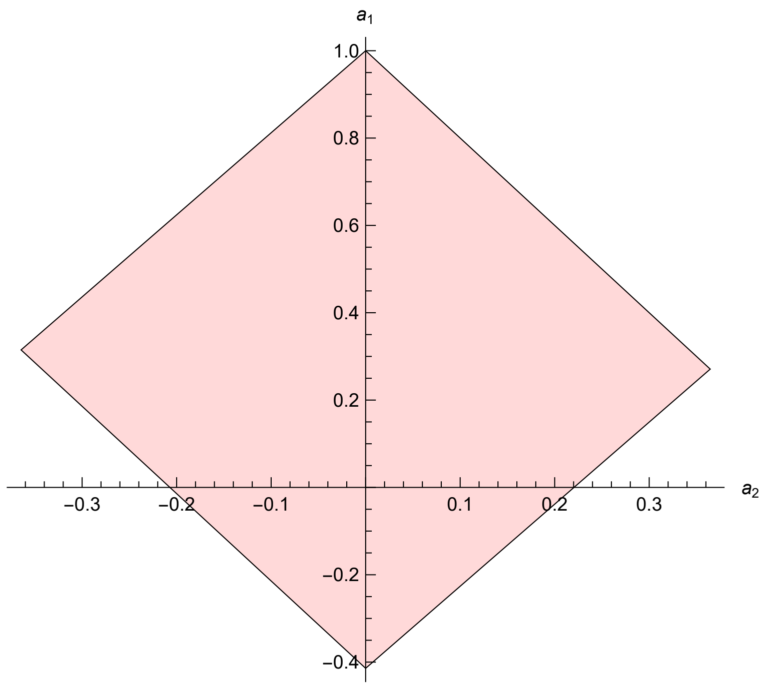

Figure 8: Stable region of symmetric system (9) with $N = 9$ and $\alpha = 0.5$

Figure 9: Stable solution of symmetric system (9) with $N = 9$, $\alpha = 0.5$, $a_1 = 0.6$, and $a_2 = -0.1$

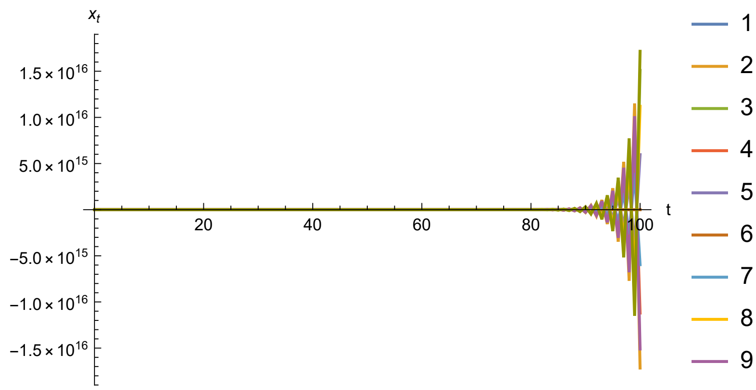

Figure 10: Unstable solution of symmetric system (9) with $N = 9$, $\alpha = 0.5$, $a_1 = 0.2$, and $a_2 = 0.6$

3.1.2. Asymmetric Case

Now, we consider the asymmetric system (9) with $a_0 = -a_2$. We define the cardioids

$$\gamma_j = \left(Re\left[e^{\iota t}\left(1 - e^{-\iota t}\right)^{\alpha}\right] + 1, \frac{1}{2\sin(2\pi j/N)} Im\left[e^{\iota t}\left(1 - e^{-\iota t}\right)^{\alpha}\right] \right), \quad j = 1, 2, \cdots, [N/2] \tag{17}$$

in the a_1a_2-plane, provided $\sin(2\pi j/N) \neq 0$.
The stability result in this case is discussed below. Note that $\lceil r \rceil$ is the ceiling function of real number r.

Theorem 3.4. *Consider the system (9) with $a_0 = -a_2$. We have following stability results:*

- *If $N = 1$ or $N = 2$ then the stable region is $1 - 2^{\alpha} < a_1 < 1$.*
- *If $N \geq 3$ is an odd number then the stable region is bounded by the line $a_1 = 1$ and the cardioid $\gamma_{\lceil \frac{N-1}{4} \rceil}$ in the a_1a_2-plane.*
- *If $N \geq 4$ is an even number then the stable region is bounded by the line $a_1 = 1$ and the cardioid $\gamma_{\lceil \frac{N}{4} \rceil}$ in the a_1a_2-plane.*

Proof: Suppose that $a_0 = -a_2$ in (9) . Therefore, the eigenvalues of the coefficient matrix A are

$$\lambda_j = a_1 + \iota 2 a_2 \sin\left(\frac{2\pi j}{N}\right), \quad j = 0, 1, \cdots, N-1. \tag{18}$$

It is observed that for $j = [N/2]+1, [N/2]+2, \cdots, N-1$, the values λ_j are complex conjugates of those for $j = 0, 1, \cdots, [N/2]$. Therefore, the stable region corresponding to λ_j is given by the cardioid γ_j defined in (17).
Since, $\lambda_0 = a_1 \in \mathbb{R}$, one of the stability conditions is

$$1 - 2^\alpha < a_1 < 1. \tag{19}$$

Further, if $N = 1$ or $N = 2$ then a_1 is the only eigenvalue of matrix A. Therefore, the stability condition is given by (19).
For $N \geq 3$, the stable region is an intersection of the cardioids γ_j and the region (19). It is observed that, this region is bounded by the "innermost" cardioid and the line $a_1 = 1$ in the a_1a_2-plane, as shown in the Figure 11. Now, we have to find the j for which the cardioid γ_j is innermost.
The innermost cardioid is generated by γ_j for which the value $\sin(2\pi j/N)$ is maximum. Further, the value $\sin(2\pi j/N)$ is maximum for the number $2\pi j/N$ which is closest to $\pi/2$ i.e. if the value $|\frac{2\pi j}{N} - \frac{\pi}{2}| = \frac{\pi}{2N}|4j - N|$ is minimum.
Thus, our problem is reduced to find minimum of the set

$$S = \{|4j - N| : j = 1, 2, \cdots, [N/2]\}. \tag{20}$$

If N is even number, then the minimum of S occurs at $j = [N/4]$. On the other hand, if N is an odd number, then the minimum of S occurs at $j = \lceil \frac{N-1}{4} \rceil$.
The result is proved.

We note that if the number of maps is multiple of 4, say $N = 4K$, $\lambda_K = a_1 + \iota 2a_2$ and $\lambda_{N-K} = a_1 - \iota 2a_2$. Also, $\lambda_0 = a_1$ for any N. The cardioid γ_K defined above reduces to cardioid for given value of α for $j = 0$ where real part is given by a_1 and imaginary part is $2a_2$. For $j = 0$, γ_j is strip between $1 - 2^\alpha \leq a_0 \leq 1$ with no condition on a_2. The stability region is given by intersection of this strip with the cardioid γ_K for given α for $N = 4K$. If N is not an exact multiple of 4, the stability region is slightly bigger and as expected it shrinks to stability region for $N = 4$ in the thermodynamic limit.

Example 3.4. *We consider the system (9) with $a_0 = -a_2$, $N = 6$ and $\alpha = 0.3$. Here, N is even and $[N/4] = 1$. According to Theorem 3.4, the stable region is bounded by the cardioid γ_1 and the line $a_1 = 1$ in the a_1a_2-plane, as shown in Figure 12. The point $a_1 = -0.3, a_2 = 0.5$ is outside the stable region and therefore we get unstable solution (cf. Figure 13). On the*

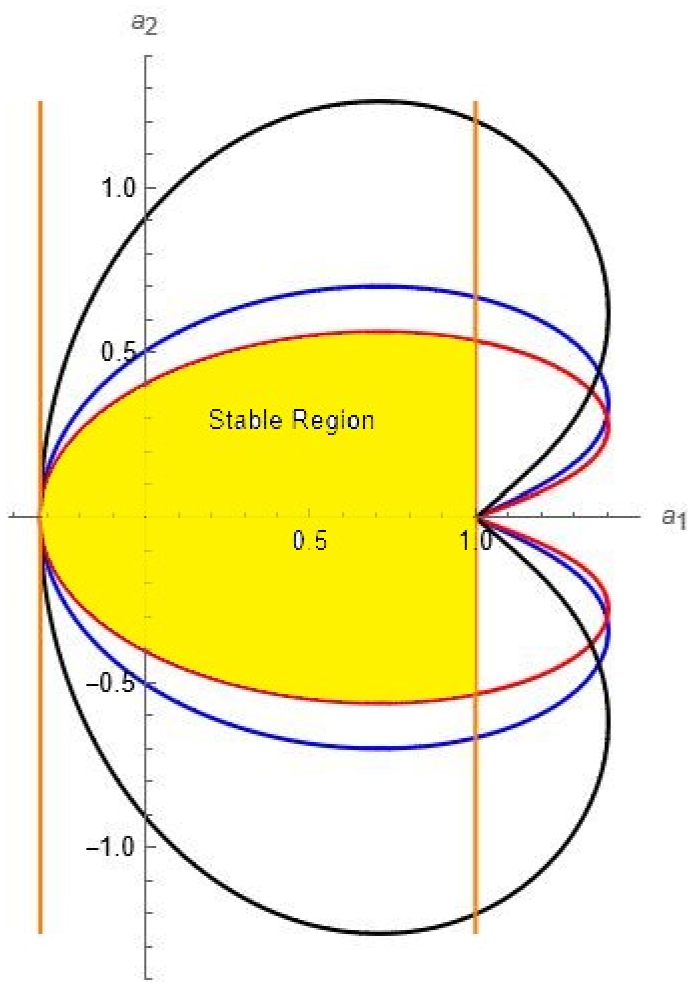

Figure 11: Stable region of asymmetric system with $a_0 = -a_2$

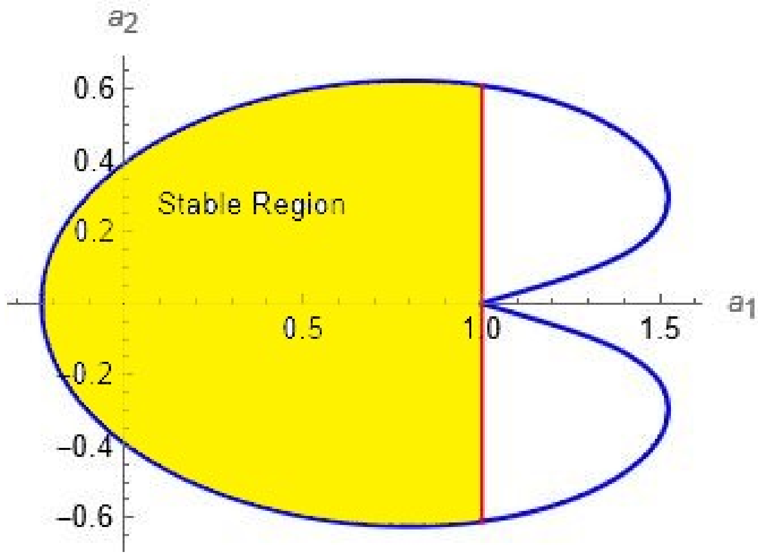

Figure 12: Stable region of system (9) with $a_0 = -a_2$, $N = 6$ and $\alpha = 0.3$

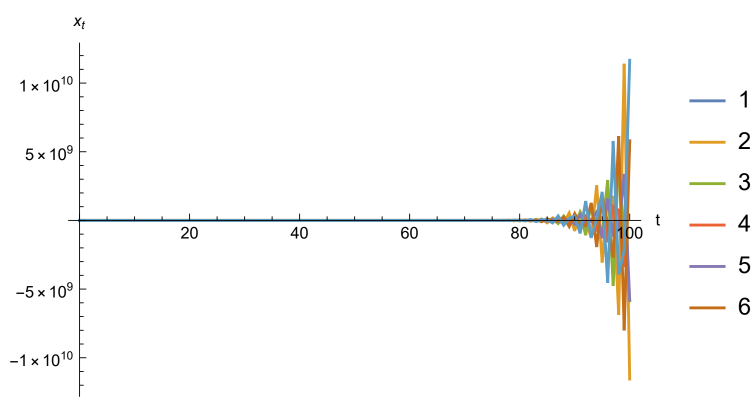

Figure 13: Unstable solution of (9) with $a_1 = -0.3, a_2 = 0.5$, $a_0 = -a_2$, $N = 6$ and $\alpha = 0.3$

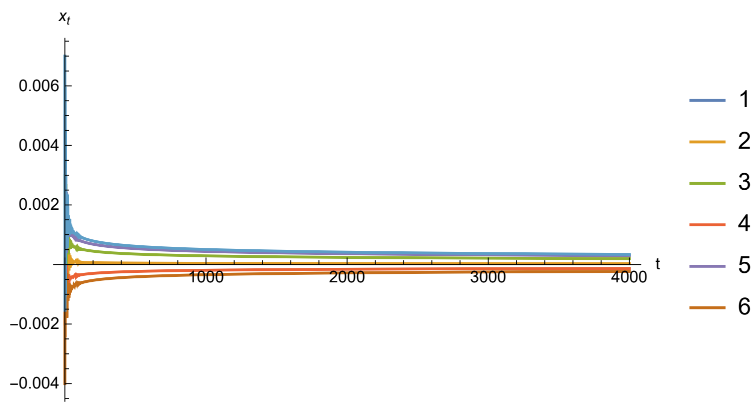

Figure 14: Stable solution of system (9) with $a_1 = -0.1, a_2 = -0.22$, $a_0 = -a_2$, $N = 6$ and $\alpha = 0.3$

other hand, we get the stable solution (cf. Figure 14) for the parameter values $a_1 = -0.1, a_2 = -0.22$.

We also verified the Theorem 3.4 for odd values of N but not presented the example for brevity.

3.1.3. Thermodynamic limit

The coupled map lattice (9) in the thermodynamic limit $N \longrightarrow \infty$ is an interesting system studied in the literature [24, 25, 26]. This limit may gives rise to some important phenomena such as rescaling of the Lyapunov spectrum [27]. The physical interpretation of this limit [28, 29] is that a coupled map lattice with a very large number of lattice points may be identified as a chain of relatively small-sized independently evolving subsystems.

As $N \longrightarrow \infty$, $\cos(\pi/N) \longrightarrow 1$. Therefore, the stable region of the symmetric system (9) in the a_1a_2-plane according to Theorem 3.3 is bounded by the quadrilateral $Q_1Q_2Q_3Q_4$ in the thermodynamic limit.

As $N \longrightarrow \infty$, the interval $[0, 2\pi]$ will contain an infinitely many values of the form $2\pi j/N$, $j = 1, 2, \cdots, N-1$. Therefore, the maximum of $\sin(2\pi j/N)$ will approach to 1 as $N \longrightarrow \infty$. Therefore, the stable region in the a_1a_2-plane of the asymmetric system (9) with $a_0 = -a_2$ according to Theorem 3.4 is bounded by the line $a_1 = 1$ and the cardioid

$$\gamma_\infty = \left(Re\left[e^{\iota t}\left(1 - e^{-\iota t}\right)^\alpha\right] + 1, \frac{1}{2} Im\left[e^{\iota t}\left(1 - e^{-\iota t}\right)^\alpha\right] \right)$$

in the thermodynamic limit.

Though we have studied 1-dimensional case in detail, the formulation is very generic and can be extended to any case where the eigenvalues of the connectivity matrix can be computed analytically. Consider a 2-dimensional case with NM maps with couplings $A_{(i,j),(i\pm1,j)} = a_0$ $A_{(i,j),(i,j\pm1)} = a_2$ $A_{(i,j),(i,j)} = a_1$. This is a block-circulant matrix with circulant blocks and the eigenvalues are given by $\lambda_{k1,k2} = a_1 + 2a_0 \cos(\theta_{k1}) + 2a_2 \cos(\theta_{k2})$ where $\theta_{k1} = \frac{2\pi k_1}{N}$ and $\theta_{k2} = \frac{2\pi k_2}{M}$. The indices k_1 and k_2 run from 0 to $N-1$ and 0 to $M-1$ respectively [30]. The bounds are given by $a_1 + 2a_0 + 2a_2$ and $a_1 - 2a_0 - 2a_2$ in the thermodynamic limit (assuming all off-diagonal couplings positive) and the stability region is given by quadrilateral where both these bounds are in the range $[-2^\alpha + 1, 1]$. Thus the formulation allows us to analytically find the stability of a coupled map lattice with any connectivity matrix if the eigenvalues can be determined analytically. If we couple each site to B nearest neighbors instead of just one neighbor or to k randomly chosen sites [31, 32] the eigenvalues of the connectivity matrix can be found analytically. The stability conditions for synchronized fixed point can be studied even in such cases. If the eigenvalues can be determined only numerically, we can still use the stability conditions to explore the stability of the system by systematically increasing the system size.

4. Fractional order coupled map lattices: Nonlinear systems

Consider the nonlinear coupled map lattice of fractional order $\alpha \in (0, 1]$

$$x_{t+1}(k) = x_0(k) + \sum_{j=0}^{t} \frac{\Gamma(t-j+\alpha)}{\Gamma(\alpha)\Gamma(t-j+1)} \left(f_0\left(x_j(k-1)\right) + f_1\left(x_j(k)\right) - x_j(k) + f_2\left(x_j(k+1)\right) \right), \tag{21}$$

where $k = 1, 2, \cdots, N$, $x_t(0) = x_t(N)$, $x_t(N+1) = x_t(1)$ and the functions $f_k : \mathbb{R} \longrightarrow \mathbb{R}$, $k = 0, 1, 2$ are continuously differentiable functions.
If we define X_t as in Section 3 and $F : \mathbb{R}^N \longrightarrow \mathbb{R}^N$ as

$$F(X_t) = \begin{bmatrix} f_0\left(x_j(N)\right) + f_1\left(x_j(1)\right) + f_2\left(x_j(2)\right) \\ f_0\left(x_j(1)\right) + f_1\left(x_j(2)\right) + f_2\left(x_j(3)\right) \\ f_0\left(x_j(2)\right) + f_1\left(x_j(3)\right) + f_2\left(x_j(4)\right) \\ \vdots \\ f_0\left(x_j(N-2)\right) + f_1\left(x_j(N-1)\right) + f_2\left(x_j(N)\right) \\ f_0\left(x_j(N-1)\right) + f_1\left(x_j(N)\right) + f_2\left(x_j(1)\right) \end{bmatrix}$$

then the system (21) is equivalent to

$$X_{t+1} = X_0 + \sum_{j=0}^{t} \frac{\Gamma(t-j+\alpha)}{\Gamma(\alpha)\Gamma(t-j+1)} \left[F\left(X_j\right) - X_j\right]. \tag{22}$$

A point $X_* = (x_*(1), x_*(2), \cdots, x_*(N))$ is called an equilibrium point of (22) if it is a fixed point of function F [33]. Therefore, such a point must satisfy

$$f_0\left(x_*(j-1)\right) + f_1\left(x_*(j)\right) + f_2\left(x_*(j+1)\right) = x_*(j), \quad j = 1, 2, \cdots, N. \tag{23}$$

For simplicity, we assume that the equilibrium point is homogeneous, i.e. $X_* = (x_*, x_*, \cdots, x_*)$ so that the conditions (23) get reduced to a single condition

$$f_0\left(x_*\right) + f_1\left(x_*\right) + f_2\left(x_*\right) = x_*. \tag{24}$$

If we identify $a_0 = f_0'\left(x_*\right)$, $a_1 = f_1'\left(x_*\right)$ and $a_2 = f_2'\left(x_*\right)$ then the linearization of (22) at homogeneous equilibrium point X_* is given by the equation (9). Furthermore, if we assume the condition (24) then all the stability results viz. Theorems 3.1, 3.2, 3.3 and 3.4 can be used to analyze the stability of X_*. We illustrate these results in the following examples.

Example 4.1. *Consider $f_1(x) = \mu x(1-x)$, the logistic map [34] and $f_2(x) = f_0(x) = 4x^3 - \delta x$.*

Here, the origin $X_* = (0, 0, \cdots, 0)$ is an equilibrium point of (22). Further, $a_1 = f_1'(0) = \mu$ and $a_0 = a_2 = f_2'(0) = -\delta$. Therefore, for $\alpha = 0.6$ and $N = 4$ the stable region in $\delta\mu$-plane is sketched in Figure 15. The stable orbits for $\mu = 0.05$, $\delta = -0.1$ are plotted in Figure 16.

Example 4.2. *We consider $f_1(x) = \mu x(1-x)$ and the circle map [35] $f_2(x) = x + \delta \sin(x)$. We also set $f_0(x) = -f_2(x)$ so that the system (22) is asymmetric.*

Again, we have origin as equilibrium X_* and $a_1 = \mu$, $a_2 = -a_0 = 1 + \delta$. We take $\alpha = 0.8$ and $N = 7$. The stable region shown in Figure 17 is bounded by the line $\mu = 1$ and the cardioid γ_2. The parameter values $\mu = 0.6, \delta = -0.8$ in the stable region give rise to stable orbits as shown in Figure 18. If we take $\mu = 1.1$ and $\delta = -1.2$ in the unstable region, then the trajectories repelled by origin are attracted by another homogeneous equilibrium point with $x_* = 1 - 1/\mu$ for the sufficiently small positive initial conditions (cf. Figure 19). Note that the trajectories will be unbounded if we take negative initial conditions, in this case.

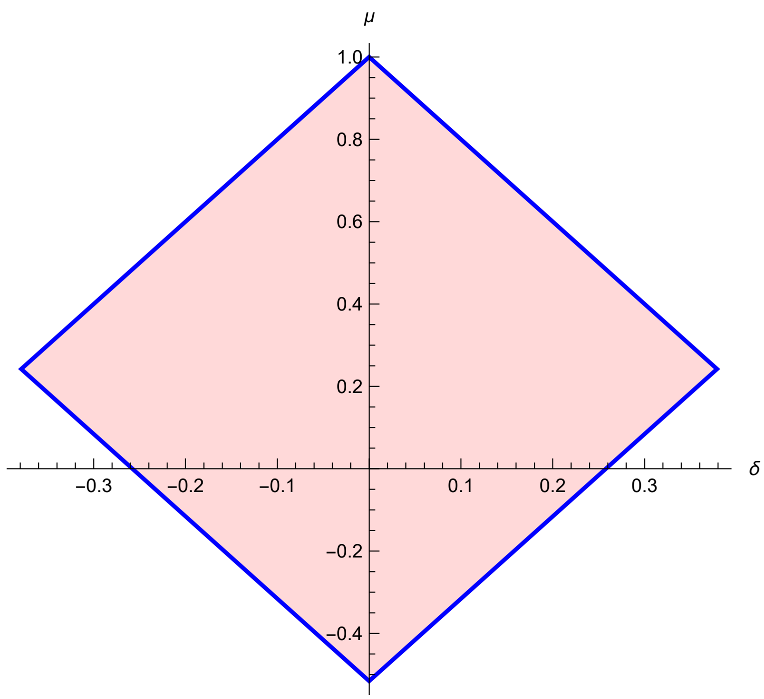

Figure 15: Stable region of origin of (22) in Ex. 4.1 with $N = 4$ and $\alpha = 0.6$

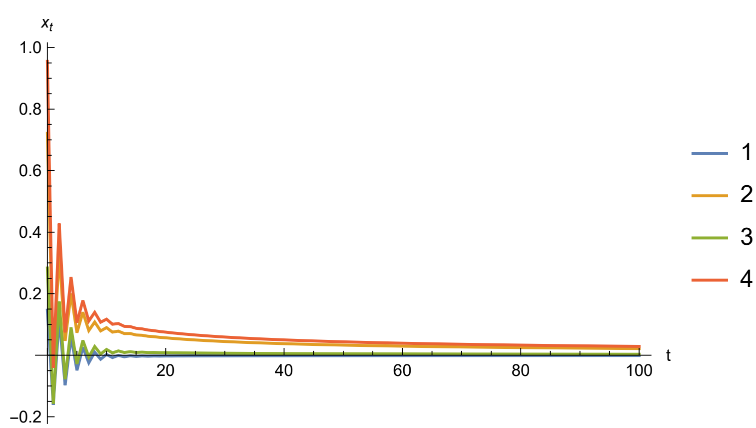

Figure 16: Stable orbits of system (22) in Ex. 4.1 with $\mu = 0.05$, $\delta = -0.1$, $N = 4$ and $\alpha = 0.6$

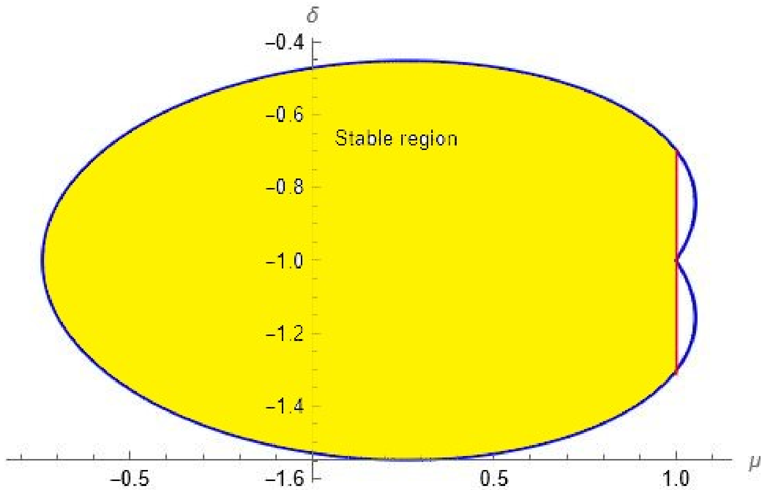

Figure 17: Stable region of origin of (22) in Ex. 4.2 with $N = 7$ and $\alpha = 0.8$

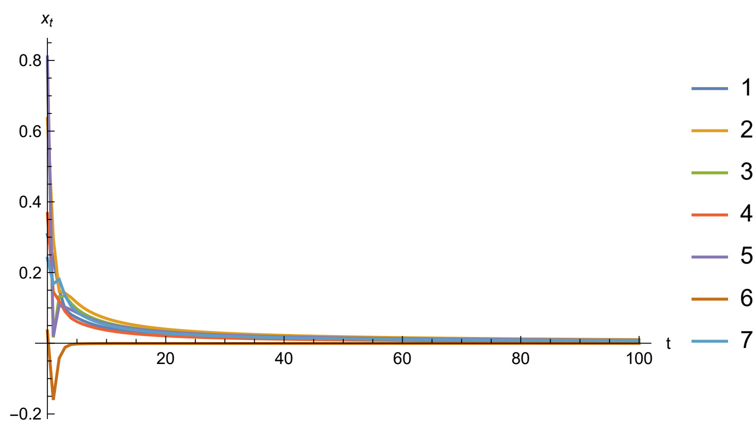

Figure 18: Stable orbits of system (22) in Ex. 4.2 with $\mu = 0.6, \delta = -0.8$, $N = 7$ and $\alpha = 0.8$

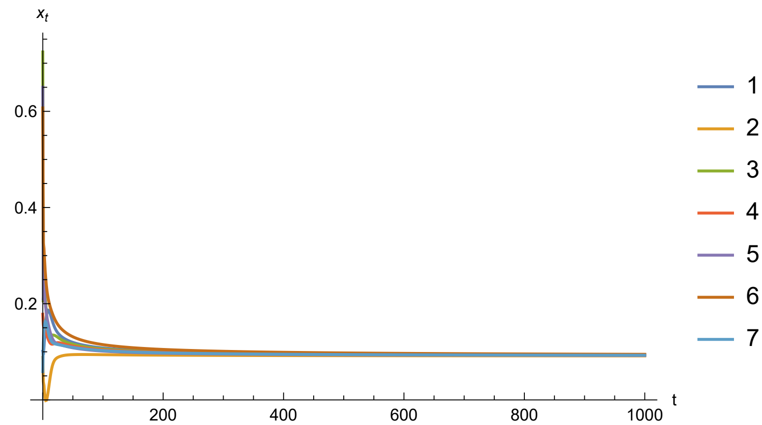

Figure 19: Orbits of system (22) in Ex. 4.2 diverging from origin for $\mu = 1.1$, $\delta = -1.2$, $N = 4$ and $\alpha = 0.6$

Example 4.3. *Consider* $f(x) = \mu x(1-x)$ *and define* $f_1(x) = (1-\epsilon)f(x)$ *and* $f_0(x) = f_2(x) = \frac{\epsilon}{2}f(x)$.

If x_* is a fixed point of f then $f(x_*) = x_*$ and hence the condition (24) is satisfied. Therefore, for this choice of functions the system (22) will have two homogeneous equilibrium points viz. $X_{1*} = (0, 0, \cdots, 0)$ and $X_{2*} = (q, q, \cdots, q)$, where $q = \frac{\mu-1}{\mu}$.

Stability of X_{1*}:

Here, $a_1 = f_1'(0) = \mu(1-\epsilon)$ and $a_2 = f_2'(0) = \epsilon\mu/2$. Therefore, $\epsilon = \frac{2a_2}{a_1+2a_2}$ and $\mu = a_1 + 2a_2$. The stable region of X_{1*} in the $\epsilon\mu$-plane can now be obtained using the Theorem 3.3 by substituting the values of a_1 and a_2 in the expressions of ϵ and μ for various values of N and α.

Stability of X_{2*}:

In this case, $a_1 = f_1'(q) = (1-\epsilon)(2-\mu)$ and $a_2 = f_2'(q) = \epsilon(2-\mu)/2$. On simplifying, we get $\epsilon = \frac{2a_2}{a_1+2a_2}$ and $\mu = 2 - a_1 - 2a_2$. The stable region of X_{2*} can now be traced in $\epsilon\mu$-plane by utilizing Theorem 3.3.

The asymmetric case $f_0(x) = -f_2(x)$ can also be done in a similar way.

5. Discussion

As mentioned above, if the eigenvalues of underlying connectivity matrix can be found analytically, the stability of the synchronized state becomes very simple even for coupled fractional maps with an altered stability condition.

One possible extension is stability analysis of spatially periodic fixed point. If an unsynchronized but spatially periodic fixed point is realized in fractional coupled maps (which is possible only in nonlinear systems), the Jacobian can be block diagonalized. These blocks have a dimension of periodicity in space [30]. This simplifies the stability analysis considerably.

Transition to a frozen or absorbing state is an extensively studied transition in nonequilibrium statistical physics which includes systems such as coupled oscillators. (Such transition is not possible in equilibrium systems because detailed balance cannot be violated.) The above work allows us to study such dynamical systems in presence of memory. The thermodynamic and asymptotic limit is important because phase can be defined only for the state of an infinite system after infinite time. The above analysis gives an analytic estimate for critical point for such system and also gives important information about the nature of instability. Of course, such systems can have a very different nature. For coupled fractional maps, a power-law decay is obtained throughout the absorbing phase and not just the critical point [36]. Thus nature of transition can be very different. In integer order maps, the bifurcation depends on whether the eigenvalue crosses the unit circle at 1, -1, or complex value [2]. It also depends on which eigenmodes become unstable [37]. Similar studies can be carried out in fractional systems.

Acknowledgment

S. Bhalekar acknowledges the University of Hyderabad for Institute of Eminence-Professional Development Fund (IoE-PDF) by MHRD (F11/9/2019-U3(A)). P. M. Gade thanks DST-SERB for financial assistance (Ref. CRG/2020/003993).

References

[1] E. Ott, Chaos in dynamical systems, Cambridge university press, 2002.

[2] S. H. Strogatz, Nonlinear dynamics and chaos with student solutions manual: With applications to physics, biology, chemistry, and engineering, CRC press, 2018.

[3] T. Bohr, P. Bak, M. H. Jensen, Transition to chaos by interaction of resonances in dissipative systems. ii. josephson junctions, charge-density waves, and standard maps, Phys. Rev. A 30 (1984) 1970–1981.

[4] J. R. Tredicce, F. T. Arecchi, G. L. Lippi, G. P. Puccioni, Instabilities in lasers with an injected signal, J. Opt. Soc. Am. B 2 (1) (1985) 173–183.

[5] D. DeTienne, G. Gray, G. Agrawal, D. Lenstra, Semiconductor laser dynamics for feedback from a finite-penetration-depth phase-conjugate mirror, IEEE J. Quantum Electron. 33 (5) (1997) 838–844.

[6] L. Glass, Cardiac arrhythmias and circle maps- a classical problem, Chaos 1 (1) (1991) 13–19.

[7] A. Tufaile, J. Sartorelli, The circle map dynamics in air bubble formation, Phys. Lett. A 287 (1) (2001) 74–80.

[8] A. Ferretti, N. Rahman, A study of coupled logistic map and its applications in chemical physics, Chem. Phys. 119 (2-3) (1988) 275–288.

[9] L. S. Storch, J. M. Pringle, K. E. Alexander, D. O. Jones, Revisiting the logistic map: a closer look at the dynamics of a classic chaotic population model with ecologically realistic spatial structure and dispersal, Theor. Popul. Biol. 114 (2017) 10–18.

[10] S. Shenoy, T. Lookman, Strain pseudospins with power-law interactions: Glassy textures of a cooled coupled-map lattice, Phys. Rev. B 78 (14) (2008) 144103.

[11] T. Yanagita, K. Kaneko, Coupled map lattice model for convection, Phys. Lett. A 175 (6) (1993) 415–420.

[12] D. A. Kessler, H. Levine, W. N. Reynolds, Coupled-map lattice model for crystal growth, Phys. Rev. A 42 (10) (1990) 6125.

[13] V. E. Tarasov, Fractional integro-differential equations for electromagnetic waves in dielectric media, Theor. Math. Phys. 158 (3) (2009) 355–359.

[14] R. Magin, Fractional calculus in bioengineering, part 1, Crit. Rev. Biomed. Eng. 32 (1) (2004).

[15] R. A. Ferreira, D. F. Torres, Fractional h-difference equations arising from the calculus of variations, Applicable Analysis and Discrete Mathematics (2011) 110–121.

[16] N. R. Bastos, R. A. Ferreira, D. F. Torres, Discrete-time fractional variational problems, Signal Processing 91 (3) (2011) 513–524.

[17] D. Mozyrska, M. Wyrwas, The z-transform method and delta type fractional difference operators, Discrete Dynamics in Nature and Society 2015 (2015).

[18] C. Fulai, L. Xiannan, Z. Yong, Existence results for nonlinear fractional difference equation, Advances in Difference Equations (2011).

[19] R. Stanisławski, K. J. Latawiec, Stability analysis for discrete-time fractional-order lti state-space systems. part i: New necessary and sufficient conditions for the asymptotic stability, Bull. Pol. Acad. Sci.: Tech. Sci. 61 (2) (2013).

[20] J. Čermák, I. Győri, L. Nechvátal, On explicit stability conditions for a linear fractional difference system, Fractional Calculus and Applied Analysis 18 (3) (2015) 651–672.

[21] P. M. Gade, S. Bhalekar, On fractional order maps and their synchronization, Fractals 29 (6) (2021) 2150150–524.

[22] M. Busłowicz, A. Ruszewski, Necessary and sufficient conditions for stability of fractional discrete-time linear state-space systems, Bulletin of the Polish Academy of Sciences. Technical Sciences 61 (4) (2013) 779–786.

[23] R. Amritkar, P. Gade, A. Gangal, V. Nandkumaran, Stability of periodic orbits of coupled-map lattices, Phys. Rev. A 44 (6) (1991) R3407.

[24] A. S. Pikovsky, J. Kurths, Collective behavior in ensembles of globally coupled maps, Physica D 76 (4) (1994) 411–419.

[25] R. Carretero-González, S. Ørstavik, J. Huke, D. Broomhead, J. Stark, Thermodynamic limit from small lattices of coupled maps, Phys. Rev. Lett. 83 (18) (1999) 3633.

[26] N. Parekh, V. Ravi Kumar, B. Kulkarni, Synchronization and control of spatiotemporal chaos using time-series data from local regions, Chaos 8 (1) (1998) 300–306.

[27] R. Carretero-Gonzalez, S. O/rstavik, J. Huke, D. Broomhead, J. Stark, Scaling and interleaving of subsystem lyapunov exponents for spatio-temporal systems, Chaos 9 (2) (1999) 466–482.

[28] K. Kaneko, Towards thermodynamics of spatiotemporal chaos, Prog. Theor. Phys. Supp. 99 (1989) 263–287.

[29] D. Ruelle, Large volume limit of the distribution of characteristic exponents in turbulence, Commun. Math. Phys. 87 (2) (1982) 287–302.

[30] P. Gade, R. Amritkar, Spatially periodic orbits in coupled-map lattices, Phys. Rev. E 47 (1) (1993) 143.

[31] P. M. Gade, C.-K. Hu, Synchronization and coherence in thermodynamic coupled map lattices with intermediate-range coupling, Phys. Rev. E 60 (4) (1999) 4966.

[32] P. M. Gade, Synchronization of oscillators with random nonlocal connectivity, Phys. Rev. E 54 (1) (1996) 64.

[33] S. S. Pakhare, S. Bhalekar, P. M. Gade, Synchronization in coupled integer and fractional-order maps, Chaos, Solitons & Fractals 156 (2022) 111795.

[34] M. Robert, Simple mathematical models with complicated dynamics, Nature 261 (1976) 459–467.

[35] L. Glass, R. Perez, Fine structure of phase locking, Physical Review Letters 48 (26) (1982) 1772.

[36] S. S. Pakhare, V. Daftardar-Gejji, D. S. Badwaik, A. Deshpande, P. M. Gade, Emergence of order in dynamical phases in coupled fractional gauss map, Chaos, Solitons & Fractals 135 (2020) 109770.

[37] R. E. Amritkar, P. M. Gade, Wavelength doubling bifurcations in coupled map lattices, Phys. Rev. Lett. 70 (1993) 3408–3411.